Fabrication of Helical Mesoporous Silica Nanostructures Using Gelators and the Mixtures with CTAC

Hiroko Hoshizawa[*1], *Masahiro Suzuki*[*1], *Hirofusa Shirai*[*1], *Kenji Hanabusa*[*1], *and Yonggang Yang*[*2]

[*1] Department of Functional Polymer Science, Faculty of Textile Science and Technology, Shinshu University, Tokida 3-15-1, Ueda 386-8567, Japan
[*2] Key Laboratory of Organic Synthesis of Jiangsu Province, College of Chemistry and Chemical Engineering, Suzhou University, Suzhou 215123, P. R. China

Abstract : Two chiral hydrogelators, L-**18ValPyBr** and D-**18ValPyBr**, composed of L- or D-valine, were synthesized. They self-assembled into thin membranes under high concentration and helical nanofibers under low concentration in pure water. Sol-gel transcription reactions were carried out under both acidic and basic conditions using the self-assemblies of these two gelators and the mixtures with CTAC as templates and TEOS as precursor. Under acidic conditions, minimum gel concentrations of L-**18ValPyBr** and D-**18ValPyBr** are very low. After sol-gel polymerization, a kind of cotton-like silica constructed by twisted mesoporous silica ribbons was obtained. These ribbons were 60 nm in width and 10 nm in thickness. Under basic conditions, both mesoporous twisted ribbons and nanotubes constructed by tightly coiled ribbons were obtained. Generally, left-handed helical structures were obtained by using L-**18ValPyBr**, while right-handed helical structures were obtained by using D-**18ValPyBr**. The morphologies were sensitive to the concentration of NH_3. When the concentration of NH_3 was 2.5 wt%, twisted ribbons were obtained. When the concentration of NH_3 was higher than 5.0 wt%, nanotubes constructed by tightly coiled ribbons were obtained. Mesoporous silica structures in nano- and micro-size were prepared by using the mixtures of L-**18ValPyBr** and CTAC under both acidic and basic conditions. Under acidic conditions, helical mesoporous fibers were obtained, and their diameter was increased with increasing the ratio of CTAC to gelator. The nanofibers obtained under basic conditions were shorter than those obtained under acidic conditions. The mesoporous channels were parallel each other and running along the axis of nanofibers.

(Received 5 August, 2008 ; Accepted 10 December, 2008)

1. Introduction

Helical structures are common in vivo, such as α-helical polypeptides and double helical DNA. Although inorganic mesoporous particles with helical morphologies or chiral mesopores are rare [1-4], the helicity and periodicity are very interesting for the potential application in chiral recognition and purification, enantiomeric catalysis, chiral sensor, and optical materials. Therefore, it is very important to find simple methods to synthesize inorganic particles with single-handed helical morphologies and chiral mesopores. Moreover, it is also essentials to control the alignment, apertures, and size of the mesopores.

For the fabrication of nanometer devices, the one-dimensional (1D) nanostructures (rod, tube, spring, and belt) are the most promising field [5]. They are easier to be aligned and self-organized into more complex structures [6]. The sol-gel transcription method [7] using gelators and lipids is a simple and powerful method to control the morphological shapes of 1D nanostructures. Especially, chiral gelators and lipids can form helical morphological shapes [8]. Up to now, the helical structures in organogel fibers [9] and self-assemblies of lipids [10] have been successfully transcribed into inorganic silica and titania. Twisted ribbons [3b], single-stranded [9, 11], double [12], and multiple helical [13] structures have been achieved using the template method. Moreover, inner-helical mesoporous nanofibers have been successfully prepared using chiral gelator [3a]. The obtained mesoporous silica nanofibers are constructed by bundles of inner-helical nanotubes which are organized in 1D.

The self-assemblies of surfactants and amphiphilic copolymers are widely used as templates to synthesize mesoporous materials. Although the mesoporous particles could be shaped into nanofibers [14] or nanoballs [15] and the mesopores could be helically chiral structures

[1-4] and the pore channels can be well-organized [16], it is still a big challenge to control the nanoparticles uniform, especially with respect to hierarchical and more complicated structures. In this paper, we focused on the assemblies formed in the mixtures of chiral gelators and a cationic surfactant as templates. Gelator may control the morphological shapes and surfactant may control the arrangement of pore channels.

2. Results and discussion

2-1 Physical properties of the chiral gelators L-18 ValPyBr and D-18ValPyBr: Chiral gelators L-**18 ValPyBr** and D-**18ValPyBr** composed of L- or D-valine are shown in Fig. 1 [17]. They are capable of causing physical gelation in both organic solvents and water; for example, THF, 1,4-dioxane, toluene, chlorobenzene, and acetonitrile. In the case of hydrogel, they are very sensitive to the pH value, that is to say, minimum gel concentrations (MGCs) are 5.0 mg/mL in 2.4 M HCl aq. and are 25 mg/mL in 11.3 wt% NH_3 aq. solution. The formation of gel is also sensitive to the cooling speed. If the hot solution is cooled very quickly, even 50 mg gelator can not gel 1.0 mL of neutral water; on the contrary, if the solution were cooled down naturally, 15 mg/mL is enough to gel water at 25℃. These results suggest that the self-aggregation of the gelator molecules is not so fast.

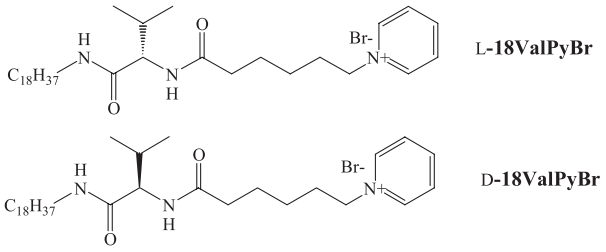

Fig. 1 Molecular structure of gelators L-**18ValPyBr** and D-**18ValPyBr**.

To visually study the superamolecular self-assemblies of gelators, we used field emission scanning electron microscope (FESEM). L-**18ValPyBr** can self-assembly into both ultrathin membranes and left-handed helical fibers in pure water (Fig. 2). In a low gelator concentration, 20 mg of L-**18ValPyBr** in 1.0 mL of water, only left-handed helical bundles were identified (Fig. 2a). On the contrary, huge membranes were predominant in a high concentration, 50 mg of L-**18ValPyBr** in 1.0 mL of water, but a few helical bundles were identified at the edges of membranes (Fig. 2b). The membranes are around 10 nm in thickness, and the helical fibers are 200-300 nm in diameter. Apparently, the helical fibers were constructed by twisted membranes. The CD spectra of L-**18ValPyBr** and D-**18ValPyBr** aggregates in pure water indicates that the molecules are packing in helix, whose sense is opposite to each other (Fig. 3). The induced CD signs from 230 nm to 280 nm maybe indicate there is a π-π interaction among the pyridinium rings.

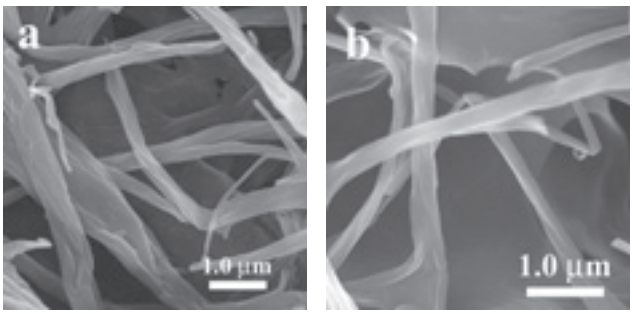

Fig. 2 FESEM images of xerogels obtained from hydrogels of L-**18ValPyBr**. (a) 20 mg of L-**18 ValPyBr** in 1.0 mL of H_2O; (b) 50 mg of L-**18 ValPyBr** in 1.0 mL of H_2O.

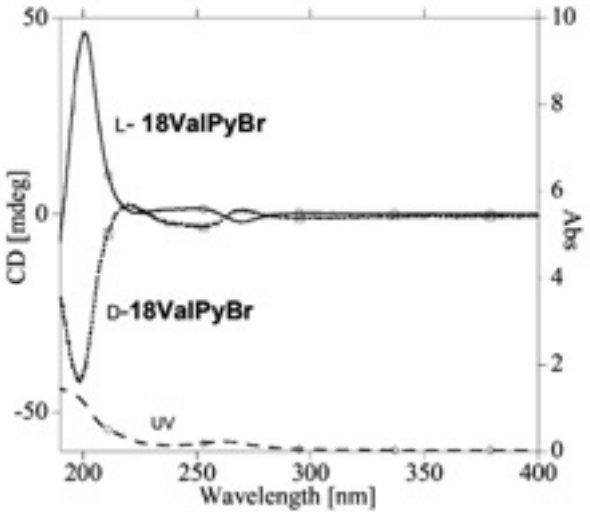

Fig. 3 CD and UV spectra of L-**18ValPyBr** and D-**18 ValPyBr** hydrogels.

2-2 Mesoporous silica nanostructures prepared under basic conditions using gelators: The synthetic procedure of silica particles was shown in the experimental part. The structures of silica particles were studied visually by FESEM and transmission electron microscope (TEM). Before taking FESEM images, 10 nm Pt-Pd was covered on the surface of samples. The morphologies of mesoporous silica were very sensitive to the preparation conditions, especially the concentration of NH_3. Generally, twisted nanoribbons were formed under lower NH_3 concentration (Fig. 4) and nanotubes were formed under higher NH_3 concentration (Fig. 5).

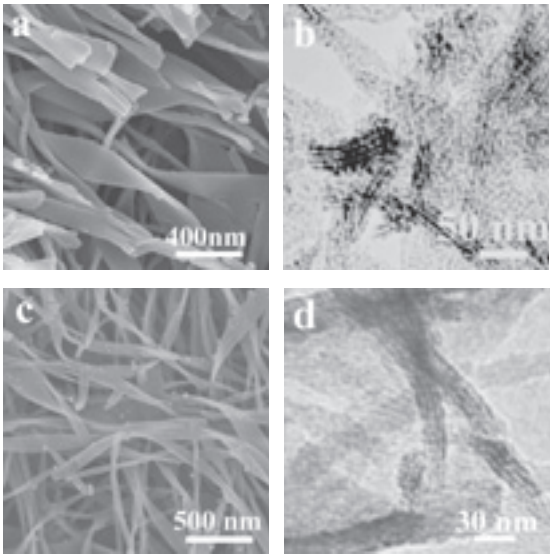

Fig. 4 FESEM (a) and TEM (b) images of left-handed twisted mesoporous silica nanoribbons obtained in a basic condition after calcination (preparation condition : 20 mg of L-**18ValPyBr**, 0.5 mL of 2.5 wt% NH_3 aq., and 50 mg of TEOS) ; FESEM (c) and TEM (d) images of right-handed twisted mesoporous silica nanoribbons obtained in a basic condition after calcination (preparation condition : 10 mg of D-**18ValPyBr**, 0.5 mL of 2.5 wt% NH_3 aq., and 20 mg of TEOS).

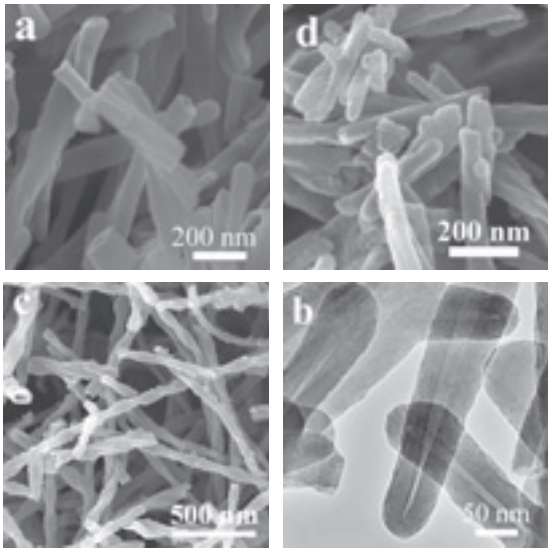

Fig. 5 FESEM (a) and TEM (b) images of nanotubes obtained in a basic condition after calcination (preparation condition: 10 mg of L-**18ValPyBr**, 1.0 mL of 5.0 % NH_3 aq., and 20mg of TEOS); FESEM (c) image of right-handed helical nanotube obtained in a basic condition after calcination (preparation condition: 10 mg of D-**18ValPyBr**, 0.50 mL of 5.0 % NH_3 aq., and 20 mg of TEOS); FESEM (d) image of nanotubes obtained in a basic condition after calcination (preparation condition: 10 mg of L-**18ValPyBr**, 0.9 mL of 5.0 % NH_3 aq., 0.1 mL of EtOH, and 20mg of TEOS).

Firstly, the sol-gel transcription reactions were carried out in 2.5 wt% NH_3 aq. (Fig. 4). Figure 4a and 4b show the FESEM and TEM images of left-handed coiled silica ribbons obtained by sol gel polymerization using the self-assemblies of L-**18ValPyBr** as templates. The obtained twisted silica ribbons are 200-300 nm in width and 10 nm in thickness. It is very interesting to find that the ribbons are constructed by bundles of nanotubes aligned in monolayer. The inner-diameter of nanotubes is ca. 4.0 nm (Fig. 4b). The existence of these ultrathin channels indicates that single strand of gel fibers acted as the template. The silica nanoribbons exhibit a nitrogen Burnauer-Emmett-Teller (BET) surface area of 224 m^2g^{-1} and a pore volume of 0.49 cm^3g^{-1}. The Barrett-Joyner-Halenda (BJH) pore size distribution plot determined from the adsorption branch shows a peak at 4.0 nm. Figure 4c and 4d show the FESEM and TEM images of right-handed coiled mesoporous silica nanoribbons obtained by using the self-assemblies of D-**18ValPyBr** as templates. The twisted silica ribbons are 200-300 nm in width. It seems that the twisted ribbons were constructed by three layers of nanotubes. Because chiral organogel fibers acted as the template, these nanotubes should have inner-helical structure. They are probably suitable for enantiomer separation and chiral catalysis.

To make mesoporous silica ribbons, the self-assemblies of surfactant [18] and lipid [19] have been used as the templates. When cationic surfactants were used, mesoporous ribbons with tracklike pore channels were obtained. The channels are oriented perpendicularly to the axis of the ribbon and are hexagonally packed together. The control of the ribbons in nano-size is still a big challenge. When a cationic lipid was used, lamellar mesostructure whose mesopores were formed among silica ribbons were obtained. The lamellar mesoporous silica ribbons are formed by the adsorption and polymerization of silica species on the surface of the self-assemblies of lipids. This mesostructure does not show high thermostability [19]. These present mesopores shown in Fig. 4 show high thermostability. The mesopores were kept even after being calcined at 550 ℃ for 5 h. The pore channels were oriented to the axis of the ribbon. Moreover, the ribbons were easy to be controlled in nano-size (Fig. 4).

On the other hand, the sol-gel transcription reactions were carried out in 5.0 and 10.0 wt% NH_3 aq. (Fig. 5a-c). The morphologies of the silica nanoparticles are sensitive the concentration of NH_3. When the concentration of NH_3 increased to 5.0 wt%, silica nanotubes constructed by tightly coiled ribbons were identified in Fig. 5a.

Unfortunately, it is hard to recognize mesopores within the ribbons from TEM image (Fig. 5b). The silica nanoribbons exhibit a nitrogen BET surface area of 474 m^2g^{-1}. The pore size distribution showed a bimodal pore structure. It is assumed that the small pores of 4-5 nm are due to the inner diameters of the pore channels. The pores larger than 20 nm are probably attributed to the inner diameters of nanotubes. When the concentration of NH_3 was increased to 10.0 wt% and the concentration of L-**18ValPyBr** was 10 mg/mL in water, viscous solution was obtained. After sol-gel polymerization, only ultrafine amorphous silica nanoparticles were obtained. However, if the concentration of L-**18ValPyBr** was increased to 25 mg/mL, both twisted ribbons and nanotubes were identified.

Hierarchical pore structures build up with different length scales can achieve highly organized functions [20]. Up to now, a variety of hierarchical mesoporous silicas involving two or three pore systems have been prepared ; for instance, ribbons [21], core-shell balls [22], and foams [23]. Generally, the hierarchical bimodal and trimodal pores structures were prepared using the mixtures of two or more templates (one-pot procedures) [24] and nanotectonic approach [25]. The nanotubes with bimodal pore structures shown here were prepared based on one-pot procedures using a single chiral cationic gelator. This result suggests that many other interesting bimodal or trimodal pore structures will be prepared using a single gelator.

The morphologies of silica nanotubes are not sensitive to the existence of ethanol. For example, when the volume ratio of water to ethanol was 9 : 1, nanotubes were obtained (Fig. 5d). However, the length of nanotubes decreased with increasing the concentration of ethanol. The formation mechanism of the mesoporous silica nanoribbons and nanotubes is illustrated in Fig. 6. First, the gelator molecules self-organize into nanofibers and then construct into ribbons. Second, TEOS oligomers adsorb on the surface of single nanofibers, aften that polymerize on the surface. Finally, after gelator molecules are removed by washing with methanol, followed by calcination, coiled mesoporous silica nanoribbons are obtained. Nanotubes are obtained when the coiled ribbons are coiled tightly.

2-3 Mesoporous silica nanostructures prepared under acidic conditions using gelators : Left-handed twisted silica nanoribbons of Fig. 7a were prepared from a mixture of 10.0 mg of L-**18ValPyBr**, 1.0 mL of 2.4 M HCl aq., and 10 mg of TEOS. This silica is cotton-like and is different from the silica obtained under basic

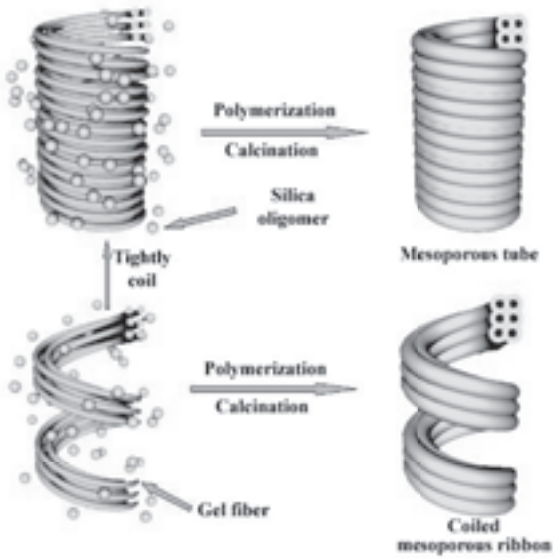

Fig. 6 Schematic representation of formation of coiled mesoporous silica nanoribbon and nanotube.

conditions. The twisted ribbons are 60 nm in width and 10 nm in thickness, which are thinner than those obtained under basic conditions. This phenomenon is due to the fact that the MGCs are different under basic and acidic conditions. Figure 7a shows that the ribbons are feasible to construct into bundles and the ribbons are nearly aligned along the same direction. This alignment is brought about by the shear force during the sol-gel transcription process. The nanoribbons obtained under acidic conditions are longer than those obtained under basic conditions. We can say that the sol-gel polymeization, in order to prepare long nanoribbons, must be carried out under acidic conditions. The nanoribbons are constructed by bundles of nanotubes in layers (Fig. 7b) under the acidic as well as the weak basic condition (Fig. 4b and Fig. 4d). We can identify more clear pore channels in silica nanostructures prepared using the self-assembly of D-**18ValPyBr** as template under an acidic condition (Fig. 7d). The channels run along the axis of nanofibers. Figure 7c shows that the right-handed coiled nanoribbons are tentative to coil tightly into nanofibers.

2-4 Mesoporous silica nanostructures prepared under acidic conditions using the mixtures of L-18ValPyBr and CTAC : Previously, for the preparation of mesoporous silica nanofibers, surfactants and amphiphilic polymers are selected as the templates and the organic liquids are used as the solvents or cosolvents [14]. The pore channels could be well-organized. However, the mesoporous fibers are often combined with small particles and it is difficult to control the fibers in nano-size, especially to obtain helical morphologies. We found that cationic gelator-direct method can get rid of small

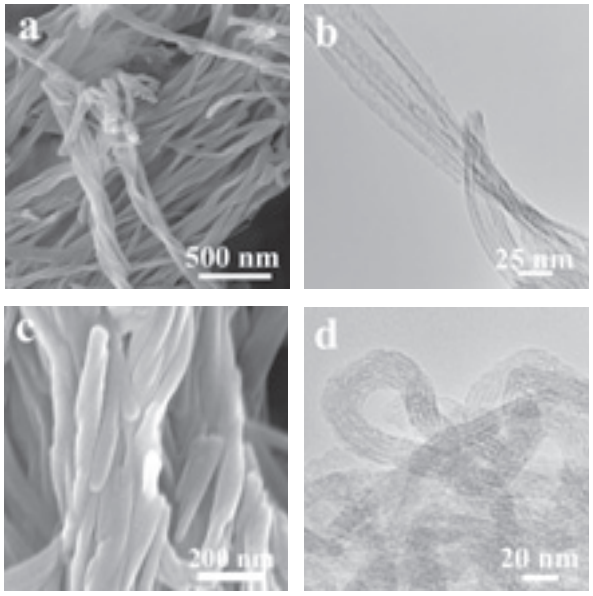

Fig. 7 FESEM (a) and TEM (b) images of left-handed twisted mesoporous nanoribbons obtained from the replication of the self-assembly of L-**18ValPyBr** under an acidic condition (preparation condition : 10 mg of L-**18ValPyBr**, 1.0 mL of 2.4 M HCl aq., and 10 mg of TEOS) ; FESEM (c) and TEM (d) images of mesoporous silica nanostructures obtained from the replication of the self-assembly of D-**18ValPyBr** under an acidic condition (preparation condition : 10 mg of D-**18ValPyBr**, 1.0 mL of 2.4 M HCl aq., and10mg of TEOS).

particles simply by keeping the concentration of gelators higher than MGCs. It seems that gelators should be the most suitable reagents to control the morphologies of mesoporous fibers.

To control the morphologies of the mesoporous particles, the mixtures of L-**18 ValPyBr** and cetyltrimethylammonium chloride (CTAC) were selected. The addition of CTAC strongly decreased the gelation ability of L-**18ValPyBr** in water. The gel fibers could be identified in the mixture of aqueous solution in optical micrograph image (Fig. 8), but they do not cause physical gel when the molar ratio of CTAC to gelator is high enough. For a better understanding the sol-gel transcription properties of the mixtures, we changed the concentration and weight ratio of them.

First, the morphologies of the mesoporous silica were controllable by changing the concentration of CTAC and gelator. When the concentration of L-**18ValPyBr** was high (10 mg of L-**18ValPyBr** and 5.0 mg of CTAC in 1.5 mL of water), huge helical bundles in 100-200 nm diameter were feasible to be constructed (Fig. 9a). The silica nanofibers exhibited a nitrogen BET surface area of 648 m^2g^{-1}. The BET pore size distribution plot determined

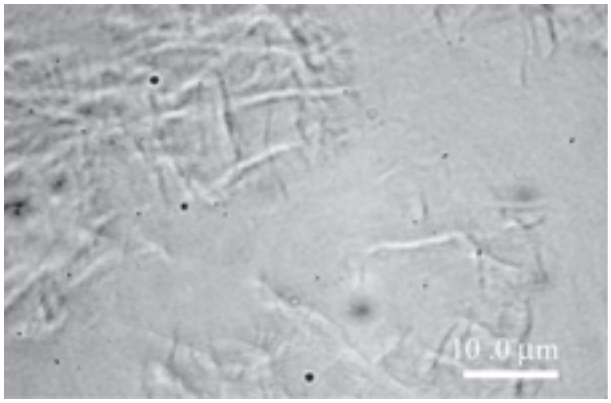

Fig. 8 Optical micrograph image of the mixture of L-**18 ValPyBr** (10.0 mg) and CTAC (20.0 mg) in water (1.0 mL)..

from the adsorption branch showed a peak at 2.7 nm. By decreasing the concentration of the reaction mixtures (10 mg of L-**18ValPyBr** and 5.0 mg of CTAC in 2.0 mL of water), the diameter of the helical bundles turned to around 100 nm (Fig. 9b). These bundles were left-handed helical. When the mixtures of D-**18ValPyBr** and CTAC were used, right-handed helical bundles were obtained (Fig. 9f).

Second, the morphologies of the mesoporous silica particles were controllable by changing the weight ratio of L-**18ValPyBr** to CTAC. Generally, when the concentration of CTAC was low, the sol-gel polymerization was carried out in gel state. Then fibrous mesoporous silica particles were obtained. For example, by gradually changing the weight ratio of L-**18ValPyBr** to CTAC from 2 : 1 to 2 : 5, the morphologies of mesoporous silica particles changed from helical bundles (Fig. 9a and 9b) to double helical nanofibers (Fig. 9c), and then to helical hexagonal rod and helical bundles in μm-size (Fig. 10c, 10d). With increasing the weight ratio of L-**18ValPyBr** to CTAC to 1 : 4, only mesoporous silica particles in micro-size could be identified (Fig. 10e). Although the morphologies of these particles were not uniform, it indicated the control of the morphology in μm-size using the mixture of gelator and cationic surfactant was possible. The silica nanofibers shown in Fig. 9c-e exhibit a nitrogen BET surface area of 736 m^2g^{-1}. The BET pore size distribution plot determined from the adsorption branch shows a peak at 2.7 nm. It seems that the surface area of mesoporous nanofibers increases with increasing the weight ratio of CTAC to L-**18ValPyBr**. Moreover, the pore channels were well-organized (Fig. 9d). When the weight ratio of CTAC to L-**18ValPyBr** is 2 : 5, helical nanofibers (Fig. 10a, b), helical hexagonal rod (Fig. 10c), and helical bundles (Fig. 10d) in μm-size were recognized. The existence of left-handed helical

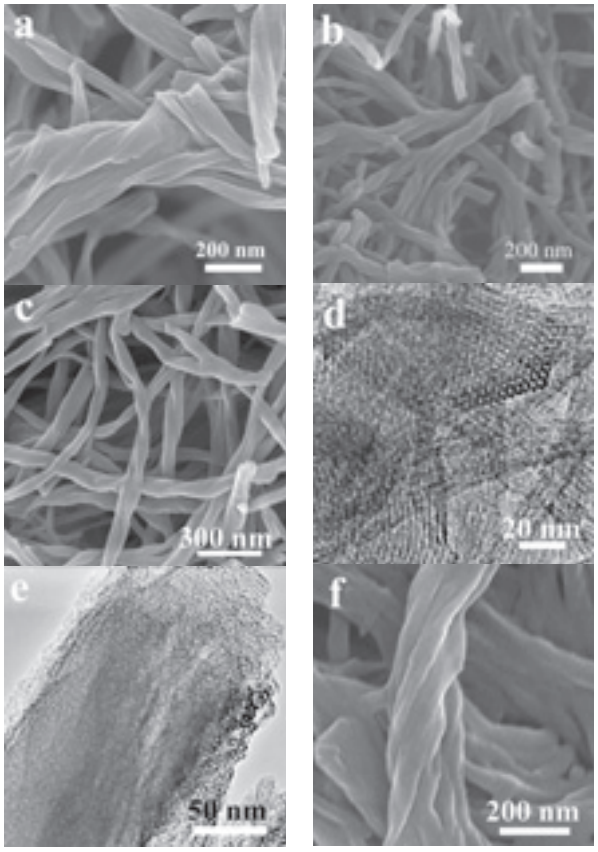

Fig. 9 FESEM (a, b, c, f) and TEM (d, e) images of the mesoporous helical silica nanostructures before calcination (preparation condition for a : 10 mg of L-**18ValPyBr**, 5.0 mg of CTAC, 1.5 mL of 2.4 M HCl aq., and 30 mg of TEOS ; preparation condition for b : 10 mg of L-**18ValPyBr**, 5.0 mg of CTAC, 2.0 mL of 2.4 M HCl aq., and 30 mg of TEOS ; preparation condition for c, d and e : 10 mg of L-**18ValPyBr**, 10 mg of CTAC, 2.0 mL of 2.4 M HCl aq., and 40 mg of TEOS ; preparation condition for f : 10 mg of D-**18ValPyBr**, 5.0 mg of CTAC, 1.5 mL of 2.4 M HCl aq., and 30 mg of TEOS).

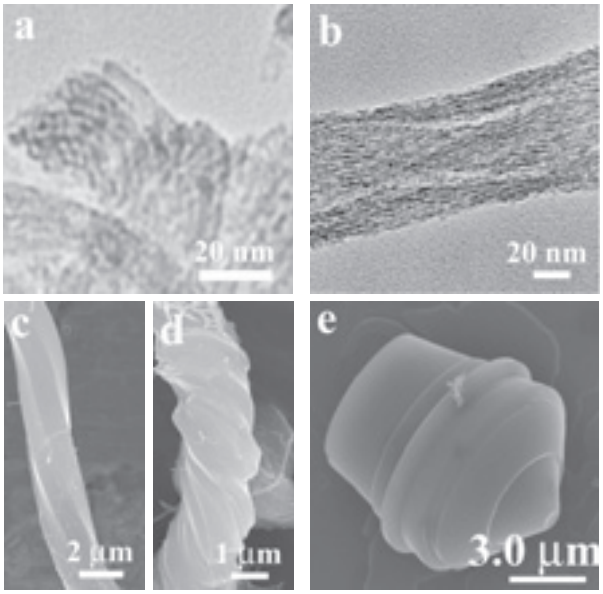

Fig. 10 FESEM (c, d, e) and TEM (a, b) images of the mesoporous silica nanostructures before calcination (preparation condition for a, b, c, and d : 10 mg of L-**18ValPyBr**, 25 mg of CTAC, 2.0 mL of 2.4 M HCl aq., and 70 mg of TEOS ; preparation condition for e : 10 mg of L-**18ValPyBr**, 40 mg of CTAC, 2.0 mL of 2.4 M HCl aq., and 100 mg of TEOS).

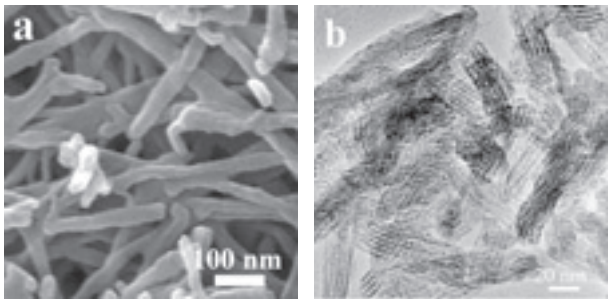

Fig. 11 FESEM (a) and TEM (b) images of silica nanofibers (preparation condition : 90 mg of L-**18ValPyBr**, 60 mg of CTAC, 4 mL of 11.3 wt% NH_3 aq., and 300 mg of TEOS).

hexagonal rods indicates that there are somewhat interaction between L-**18 ValPyBr** and CTAC. L-**18ValPyBr** could increase the length of CTAC micelle.

2-5 Mesoporous silica nanostructures prepared under basic conditions using the mixtures of L-18ValPyBr and CTAC : Although silica nanofibers could be prepared under basic conditions using the mixture of L-**18ValPyBr** and CTAC, generally, the nanofibers were not helical (Fig. 11). Slightly helical morphologies were only identified when the weight ratio of L-**18ValPyBr** to CTAC was higher than 6.5 : 1. The nanofibers shown in Fig. 11 were prepared under the ratio of L-**18ValPyBr** to CTAC 1.5 : 1. The obtained nanofibers were 20 nm in diameter and several hundreds of nanometer in length. The pore channels were parallel each other and running along the axis of the nanofibers (Fig. 11a and 11b). The untrafine structure indicated high outer-surface area. The N_2 adsorption isotherm gave a BET surface area of 844 m^2g^{-1} and a pore volume of 1.32 cm^3g^{-1}. The BJH pore size distribution plot determined from the adsorption branch showed a peak at 3.0 nm.

Although many groups have successfully prepared mesoporous nanoparticles, special apparatus, dilute conditions, and organic solvents were essential [15, 26]. Only a few papers showed ultra-fine nanoparticles less then 50 nm in diameter [15]. However, the mesopores were often disordered and the morphologies were not controllable. The prepartion of unltrafine mesoporous particles using the mixtures of gelator and surfactant will

partially solve this problem. Moreover, we can expect the pore channels are inner helical [27].

3. Conclusions

The sol-gel transcription reaction using gelator and the mixtures of gelator and cationic surfactant is a powerful method to control the order and structure of mesopores and the morphologies of the particles in nano- and micro-size. Here we successfully prepared mesoporous twisted silica nanoribbons, nanotubes, helical mesoporous silica fibers in nano- and micro-size as well as ultrafine mesoporous silica nanofibers using chiral gelators and the mixture with CTAC under basic and acidic conditions. According to this method, the morphologies of mesoporous particles and the structure of mesopores are controllable.

4. Experimental

4.1 Synthesis of gelators

L-**18ValPyBr** and D-**18ValPyBr** were synthesized according to the previous research [18].

4.2 Preparation of twisted mesoporous silica nanoribbons under basic conditions

A typical synthetic procedure was shown as follows : L-**18ValPyBr** (20 mg, 0.032 mmol) was dissolved in 0.5 mL of 2.5 % NH_3 aq., and then 50 mg (0.24 mmol) of TEOS was dropped into the solution under strongly stirring at room temperature. After the reaction mixture turned white, stirring was stopped. The gel was kept at room temperature for 1 day and 80 ℃ for 4 days under static conditions. After that the gelator was removed by rinse with a mixture of 100 mL of methanol and 5 mL of 36.0 % HCl aq. for 1 h and then dried in air. Finally, calcination was performed at 250 ℃ for 2 h and 550 ℃ for 5 h under aerobic condition.

4.3 Preparation of twisted mesoporous silica nanoribbons under acidic conditions

A typical synthetic procedure was shown as follows : L-**18ValPyBr** (10 mg, 0.016 mmol) was dissolved in 2.0 mL of 2.4 M HCl aq., and then 20 mg (0.096) of TEOS was dropped into the solution and strongly stirred at hot temperature. After the reaction mixture turned to transparent, stirring was stopped. Opaque gel was formed during the mixture cooling down to room temperature. After being kept at room temperature for 1 day and 80 ℃ for 4 days under static conditions, the gelator was removed by rinse with a mixture of 100 mL of methanol and 5 mL of 36 % HCl aq. for 1 h. And then the result material was dried in air.

4.4 Preparation of helical mesoporous silica nanofibers under acidic conditions using the mixtures of gelator and CTAC

A typical synthetic procedure was shown as follows : L-**18ValPyBr** (10 mg, 0.016 mmol) and CTAC (5 mg, 0.016) was dissolved in 1 mL of 2.4 M HCl aq., and then 30 mg (0.14 mmol) of TEOS was dropped into the solution and strongly stirred at room temperature until a transparent solution was formed. Opaque gel was formed around 3 min later after stopping stirring. The gel was kept at room temperature for 1day and 80 ℃ for 4 days under static condition. Finally, the gelator was removed by rinse with a mixture of 100 mL of methanol and 5 mL of 36.0 % HCl aq. for 1 h.

4.5 Preparation of mesoporous silica nanofibers under basic conditions using the mixtures of gelator and CTAC

A typical synthetic procedure was shown as follows : L-**18ValPyBr** (120 mg, 0.19 mmol) and CTAC (30 mg, 0.094 mmol) was dissolved in 4 mL of 11.3 % NH_3 aq., and then 300 mg (1.44 mmol) of TEOS was dropped into the solution under strongly stirring at 0 ℃. Opaque gel was formed 2 mins later. The gel was kept at room temperature for 1 day and 80 ℃ for 4 days under static condition. After that the gelator was removed by rinse with a mixture of 100 mL of methanol and 5 mL of 36.0 % HCl aq. for 1 h and then dried in air. Finally, calcination was performed at 250 ℃ for 2 h and 550 ℃ for 5 h under aerobic condition.

Characterization : FT-IR spectrum was taken on a Jasco FS-420 spectrometer. ^{1}H-NMR spectra were recorded with a Bruker AVANCE 400 spectrometer using TMS as an internal standard. Elemental analyses were performed on a Perkin Elmer series II CHNS/O analyzer 2400. TEM images were obtained using a JEOL JEM-2010. Field emission scanning electron microscopy (FE-SEM) was taken on a Hitachi S-5000. Circular dichronism (CD) spectra were measured on a JASCO J 650 spectrophotometer (cell diameter 0.1 mm). Specific surface area and pore-size distribution were determined by the BET and BJH methods, using a N_2 adsorption isotherm measured by a Shimadzu Gemini 2375 instrument.

Acknowledgements

This work was supported by Grant-in-Aid for The Global COE Program by the Ministry of Education, Culture, Sports, Science and Technology of Japan.

References

1. a) T. E. Gier, X. Bu, P. Feng, and G. D. Stucky, *Nature*, **395**, 154 (1998). b) Y. Wu, G. Cheng, K. Katsov, S. W. Sides, J. Wang, J. Tang, G. H. Fredrickson, M. Moskovits, and G. D. Stucky, *Nat. Mater.,* **3**, 816 (2004).
2. a) S. Che, Z. Liu, T. Ohsuna, K. Sakamoto, O. Terasaki, and T. Tatsumi, *Nature*, **429**, 281 (2004). b) T. Ohsuna, Z. Liu, S. Che, and O. Terasaki, *Small*, **1**, 233 (2005).
3. a) Y. Yang, M. Suzuki, A. Kurose, H. Shirai, and K. Hanabusa, *Chem. Commun.,* 2032 (2005). b) Y. Yang, M. Suzuki, O. Sanae, H. Shirai, and K. Hanabusa, *Chem. Commun.,* 4462 (2005).
4. Y. Yang, M. Suzuki, H. Fukui, H. Shirai, and K. Hanabusa, *Chemistry of Materials*, **18**, 1324 (2006).
5. Z. L. Wang, *Adv. Mater.,* **12**, 1295 (2000).
6. Y. Xia, P. Yang, Y. Sun, Y. Wu, B. Mayers, B. Gates, Y. Yin, F. Kim, and H. Yan, *Adv. Mater.,* **15**, 353 (2003).
7. Y. Ono, K. Nakashima, M. Sano, Y. Kanekiyo, K. Inoue, J. Hojo, and S. Shinkai, *Chem. Commun.,* 1477 (1998).
8. K. Hanabusa, M. Yamada, M. Kimura, and H. Shirai, *Angew. Chem. Int. Ed.,* **35**, 1949 (1996).
9. J. H. Jung, Y. Ono, K. Hanabusa, and S. Shinkai, *J. Am. Chem. Soc.,* **122**, 5008 (2000).
10. A. M. Seddon, H. M. Patel, S. L. Burkett, and S. Mann, *Angew. Chem. Int. Ed.,* **41**, 2988 (2002).
11. S. Kobayashi, N. Hamasaki, M. Suzuki, M. Kimura, H. Shirai, and K. Hanabusa, *J. Am. Chem. Soc.,* **124**, 6550 (2002).
12. J. H. Jung, K. Yoshida, and T. Shimizu, *Langmuir*, **18**, 8724 (2002).
13. S. Tamary, M. Takeuchi, M. Sano, and S. Shinkai, *Angew. Chem. Int. Ed.,* **41**, 853 (2002).
14. a) H. Yang, N. Coombs, and G. A. Ozin, *Nature*, *386*, 692 (1997). b) S. Schacht, Q. Huo, I. G. Voigt-Martin, G. D. Stucky, and F. Schüth, *Science*, **273**, 768 (1996). c) S. Mann, and G. A. Ozin, *Nature*, **382**, 313 (1996). d) F. Marlow, B. Spliethoff, B. Tesche, and D. Zhao, *Adv. Mater.,* **12**, 961 (2000). e) F. Kleitz, F. Marlow, G. D. Stucky, and F. Schüth, *Chem. Mater.,* 13, 3587 (2001).
15. Y. Lu, H. Fan, A. Stump, T. L. Ward, T. Rieker, and J. Brinker, *Nature*, **398**, 223 (1999).
16. J. Wang, C.-K. Tsung, R. C. Hayward, Y. Wu, and G. D. Stucky, *Angew. Chem. Int. Ed.,* **44**, 332 (2005).
17. M. Suzuki, S. Owa, M. Kimura, A. Kurose, H. Shirai, and K. Hanabusa, *Tetrahedron Lett.,* **46**, 303 (2005).
18. J. Wang, C.-K. Tsung, R. C. Hayward, Y. Wu, and G. D. Stucky, *Angew. Chem. Int. Ed.,* **44**, 332 (2005).
19. A. M. Seddon, H. M. Patel, S. L. Burkett, and S. Mann, *Angew. Chem. Int. Ed.,* **41**, 2988 (2002).
20. M. Antonietti and G. A. Ozin, *Chem. Eur. J.,* **10**, 28 (2004).
21. G. Larsen, S. Noriega, R. Spretz, and R. Velarde-Ortiz, *J. Mater. Chem.,* **14**, 2372 (2004).
22. S. Areva, C. Boissière, D. Grosso, T. Asakawa, and C. Sanchez, M. Lindén, *Chem. Commun.,* 1630 (2004).
23. a) L. Huerta, C. Guillem, J. Latorre, A. Beltrán, D. Beltrán, and P. Amorós, *Chem. Commun.,* 1448 (2003). b) K. Suzuki, K. Ikari, and H. Imai, *J. Mater. Chem.,* **13**, 1812 (2003).
24. D. Kuang, T. Brezesinski, and B. Smarsly, *J. Am. Chem. Soc.,* **126**, 10534 (2004).
25. S. A. Davis, M. Breulmann, K. H. Rhodes, B. Zhang, and S. Mann, *Chem. Mater.,* **13**, 3218 (2001).
26. a) R. I. Nooney, D. Thirunavakkarasu, Y. Chen, R. Josephs, and A. E. Ostafin, *Chem. Mater.,* **14**, 4721 (2002). b) C. E. Fowler, D. Khushalani, B. Lebeau, and S. Mann, *Adv. Mater.,* **13**, 649 (2001).
27. J. H. Jung, S. Shinkai, and T. Shimizu, *Chem. Mater.,* **15**, 2141 (2003).